Tellus (2000), 52B, 1013–1024
Printed in UK. All rights reserved

TELLUS
ISSN 0280–6509

Annual carbon fluxes in the upper Greenland Sea based on measurements and a box-model approach

By L. G. ANDERSON[1]*, H. DRANGE[2], M. CHIERICI[1], A. FRANSSON[1], T. JOHANNESSEN[3], I. SKJELVAN[3] and F. REY[4], [1]*Analytical and Marine Chemistry, Göteborg University, SE-412 96 Göteborg, Sweden;* [2]*Nansen Environmental and Remote Sensing Center, Edvard Griegsvei 3A, N-5059 Bergen, Bergen, Norway;* [3]*Geophysical Institute, University of Bergen, Allegaten 70, N-5007 Bergen, Norway;* [4]*Institute of Marine Research, PO Box 1870-Nordnes, N-5024 Bergen, Norway*

(Manuscript received 9 December 1998; in final form 29 October 1999)

ABSTRACT

Measurements of nitrate and the carbonate system parameters performed mainly from 1993 to 1997 have been used to estimate the evolution of the concentration fields over the year in the surface and underlying waters of the central Greenland Sea. This, together with synoptic surface wind data from the NCEP/NCAR reanalysis project, is used to evaluate the vertical mixing, the biological production and decay, as well as the air–sea exchange of CO_2 in the region. In the winter season, the vertical mixing dominates the change of the nitrate concentration in the surface water. The mixing factor estimated for this season is used to compute the addition of chemical constituents to the surface water from below. The residual nitrate concentration change, after the mixing contribution has been subtracted, is attributed to biological production or decay. The computations are performed with a 1-day resolution and initially the advective contribution is neglected, as the horizontal gradients in the central Greenland Sea gyre are small. Following this approach, the air–sea flux of CO_2 is directed into the sea all year around, with an annual uptake of 53 ± 4 g C m^{-2} yr^{-1} for the years 93 to 97. The carbon flux as driven by biology shows a strong primary production peak around Julian day 140 followed by a decrease which turns into decay of organic matter at about day 200. Summarizing the biological activity in the surface water over the year gives a new production of 34 g C m^{-2} yr^{-1}. The vertical flux of dissolved inorganic carbon into the surface water from below amounts to 11 g C m^{-2} yr^{-1}. The build up of carbon in the surface water, 30 g C m^{-2} yr^{-1}, is explained by that the temperature of the outflowing water is approximately 2°C colder than the inflowing water, giving a higher dissolved inorganic carbon concentration as a result of the increase in the solubility of carbon dioxide with lower temperatures. The uncertainties in the above stated numbers are $\pm 20\%$.

1. Introduction

The Greenland Sea is a region of deep water formation and as such transports chemical constituents from the surface to the deep ocean. This deep water formation has been mentioned as a significant sink of anthropogenic carbon dioxide, i.e., carbon dioxide produced by human activities like deforestation and fossil fuel burning. The role of the oceans in taking up anthropogenic carbon dioxide and the processes that control the air–sea exchange of carbon dioxide has been given much attention (Volk and Hoffert, 1985; Siegenthaler and Sarmiento, 1993; Stocker et al., 1994). The deep convection areas, where water in contact with the atmosphere gains a density high enough to sink and form deep water, tends to bring carbon

* Corresponding author.
e-mail: leif@amc.chalmers.se

dioxide away from contact with the atmosphere. This newly formed deep water will thus carry the anthropogenic CO_2 to the deep oceans.

The Greenland Sea deep water (GSDW) is a relatively young water mass as deduced from its content of anthropogenic tracers such as tritium, helium, argon, krypton, and CFCs (Rhein, 1991; Schlosser et al., 1991; Bönisch and Schlosser, 1995; Bönisch et al., 1997). In order to explain the measured chloro-fluoro-carbon (CFC) data in the Greenland Sea, Anderson et al. (1999) applied a ventilation model giving an annual renewal by deep water formation of around 1% below 1500 m, corresponding to a mean ventilation of 0.17 ± 0.05 Sv. This ventilation gave a sequestering of anthropogenic carbon dioxide, which in 1995 equaled $2.4 \pm 0.7 \times 10^{12}$ g C yr^{-1}.

Carbon is also transported from the surface to the abyss by the biological pump, i.e., biologically produced particles, both living plankton and dead organic matter. The new production in the Greenland Sea has been reported to 57 g C m^{-2} yr^{-1} (Noji et al., 1996). Of this new production, 1.7 g C m^{-2} yr^{-1} is found as total organic carbon in sediment traps at both around 1000 and 2000 m depth (Noji et al., 1996). An additional flux of carbon is attributed to vertical migration of zooplankton to deep waters (down to 2000 m) during the winter season, which can add a net flux of 3.5 g C m^{-2} yr^{-1} (Noji et al., 1996). Furthermore, dissolved organic carbon can be transported from the surface layer in the fall by vertical mixing with DOC-poor underlying waters (Carlson et al., 1994).

The different surface water processes are essential for both the physically and biologically mediated vertical carbon flux. These processes are seasonal, with cold winters of low biological activity and relatively warm summers with high biological activity. In this work we investigate the seasonal evolution of nitrate and dissolved inorganic carbon in the surface water during the mid 1990s and apply a box model to elucidate the carbon fluxes by air–sea exchange, biological activity and vertical mixing to and from this surface water.

2. Analytical methods

Nitrate was determined using a standard spectrophotometric technique (Grasshoff, 1983). The precision and accuracy of the nitrate determination should be significantly higher than the variability within the data set of each cruise.

All total dissolved inorganic carbon (C_T) determinations were performed by gas extraction from acidified samples followed by coulometric titration (Johnson et al., 1985; 1987). The precision was better than ± 1 μmol kg^{-1}, determined as the standard deviation of replicate analyses on samples. The accuracy was set by running a certified reference material supplied by A. Dickson (Scripps Institution of Oceanography, USA) at each change of cell solution. The precision when analysing the reference water was the same as for samples, and the ratio of the certified concentration to the measured was used to correct the seawater samples. The absolute correction was less than 20 μmol kg^{-1} and as the sample concentration and that of the reference water deviated less than 200 μmol kg^{-1}, this one point calibration should be sufficient for the accuracy to be within double the precision.

Total alkalinity (A_T) was determined by titrating the samples with 0.1 M HCl and measuring the change in pH with a potentiometric method (Haraldsson et al., 1997). The estimate of precision for A_T followed the same procedures as for C_T, and was better than ± 2 μmol kg^{-1} during all cruises. Also the accuracy for A_T was determined by analysing the Dickson reference material for all cruises after 1995, when it was certified for A_T. As the precision when running the reference material was the same as when analysing samples, the accuracy should be within double that of the precision.

3. Data

The data used in this evaluation was collected during the European Subpolar Program (ESOP) and complemented by a few nitrate data available from ICES data centre (Table 1). All data used were collected in the central Greenland Sea (73 to 78°N and 15°W to 5°E, Fig. 1). The mean profiles in the upper 200 m of nitrate, normalized C_T and normalized A_T for the different cruises are presented in Fig. 2.

For the evaluation of the seasonal variability of the total dissolved inorganic carbon concentration and total alkalinity, data were collected in the

Table 1. *Cruise information*

Expedition	Time (Julian day)	NO_3^-	C_T
Hakon Mosby, 1994	50	y	y
Hakon Mosby, 1995	55	n	y
Hakon Mosby, 1997	70	y	y
Hakon Mosby, 1994	70	y	y
Johan Hjort, 1997	105	n	y
Johan Hjort, 1993	125	y	n
Johan Hjort, 1995	135	y	y
Johan Hjort, 1994	150	y	y
James Clark Ross, 1996	180	y	y
Johan Hjort, 1993	220	y	y
Johan Hjort, 1998	225	n	y
BS, 1972	235	y	n
Johan Hjort, 1995	315	y	y
Hakon Mosby, 1996	315	y	y

Julian days during which the data used in this work were collected, with the notation y (yes) and n (no) indicating whether nitrate and/or total dissolved inorganic carbon (C_T) were determined.

time period 1993 to 1997. Using only these recent data for the carbonate system has two advantages, one being that the analytical technique has developed significantly during the last 10 years (introduction of the coulometric technique and the availability of reference material, Dickson and Goyet, 1994) and the second that a short time period minimizes the problem with the time-dependent anthropogenic contribution. Total alkalinity is not affected by this anthropogenic contribution. The concentration of A_T normalized to a salinity of 35 is fairly constant over the year, 2293 ± 12 μmol kg^{-1} ($n = 219$) in the surface water (Fig. 2c). The normalized C_T concentration on the other hand shows a seasonal trend in the top 30 m (Fig. 3a). From the fit to the normalized C_T and the constant normalized A_T together with a fit to the observed salinity, the C_T and A_T concentration functions were computed. These in turn were used together with salinity and temperature to calculate the fugacity of carbon dioxide (fCO_2, Fig. 3b) using the carbonate system speciation program of Lewis and Wallace (1998).

In order to evaluate the air–sea flux of CO_2, the difference in fCO_2 between the atmosphere and the surface mixed layer, as well as the wind speed was needed. The atmospheric fCO_2 was taken in 1992 from weather station "Mike" in the Norwegian Sea (Conway et al., 1994), while the

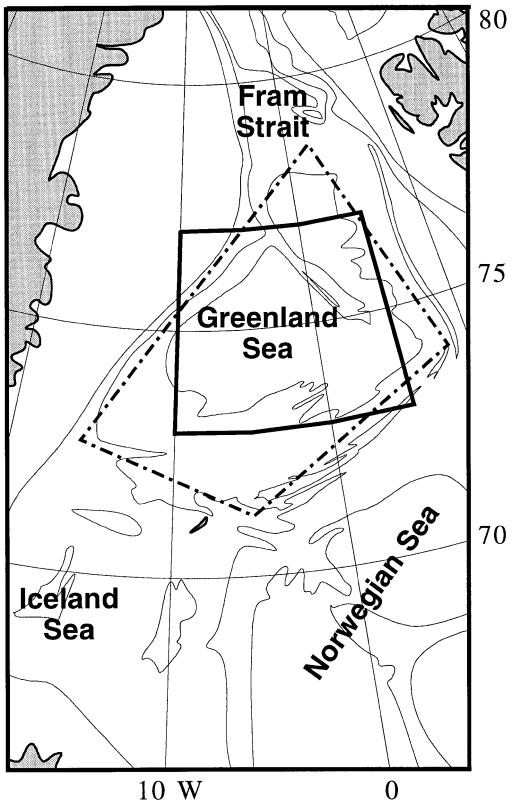

Fig. 1. Map of the Greenland Sea. The data have been collected in the area within the solid line. The area used for the computation of the total fluxes is within the dotted line.

wind speed for years 1993 to 1997 (Fig. 3c) was taken from the synoptic surface wind data within the NCEP/NCAR reanalysis project (Kalnay et al., 1996).

4. The model computations

For the evaluation of the fluxes we apply a simple box model (schematically illustrated in Fig. 4). The model follows the concentration changes in the surface water over a year with time steps of one day. In the initial state we assume that the horizontal in- and out-flux are balanced. To avoid the problem with varying depth of the surface mixed layer we compute the deficit in the top 150 m, relative to the mean concentration in the subsurface water (150 to 300 m). This is done

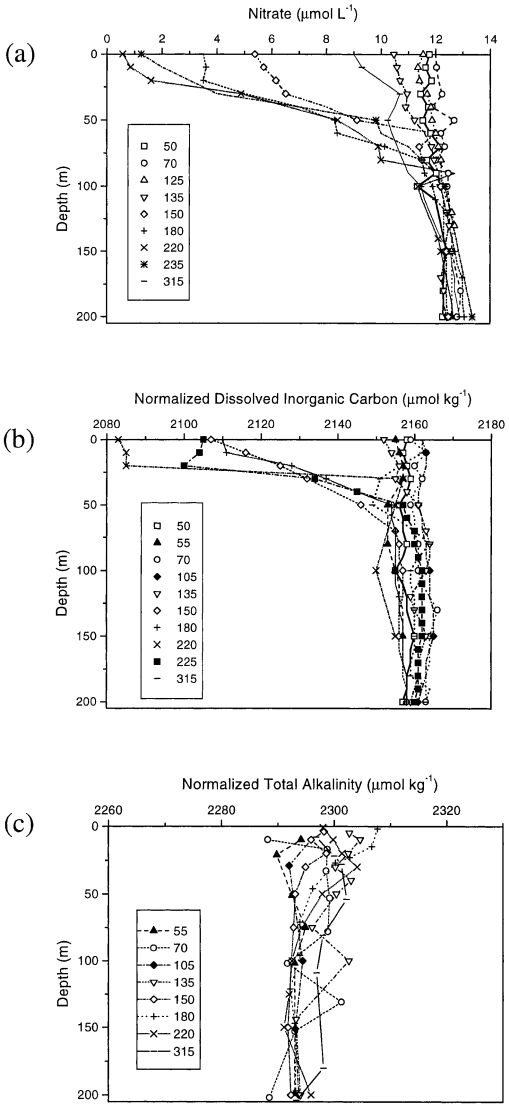

Fig. 2. Mean depth profiles of (a) nitrate, (b) total dissolved inorganic carbon (normalized to a salinity of 35) and (c) total alkalinity (normalized to a salinity of 35) for each cruise in the upper 200 m of the central Greenland Sea. The numbers indicate the average Julian day of observations.

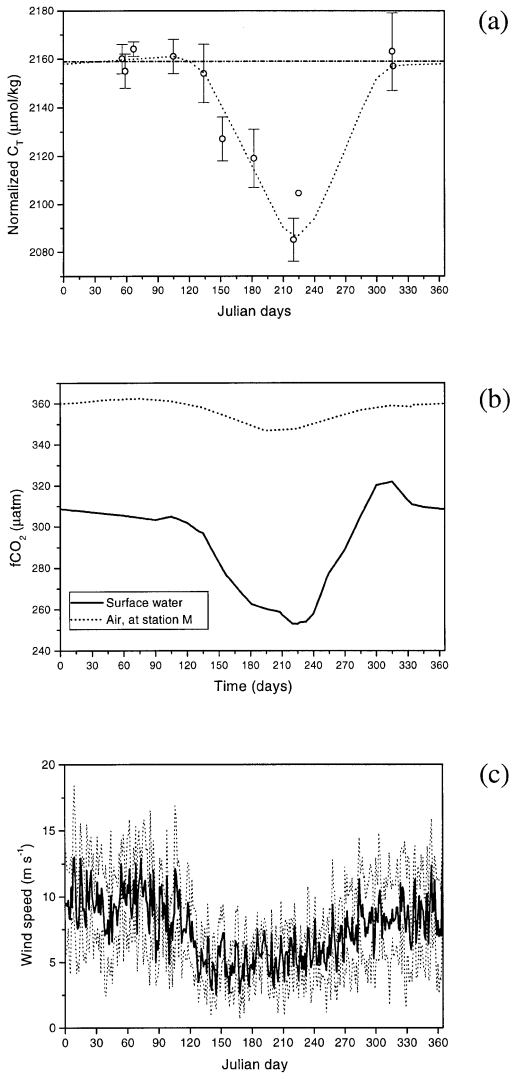

Fig. 3. The average properties in the top 30 m of (a) total dissolved inorganic carbon, normalized to a salinity of 35 (NC_T), (b) fCO_2 computed from NC_T, total alkalinity, salinity, temperature and phosphate concentrations, together with the atmospheric record from weather ship "Mike", and (c) the synoptic 24-h surface wind (mean, solid line, ±standard deviations, dotted lines, for the years 1993 to 1997).

by subtracting the concentration (mol m^{-3}) at every 10 m interval between the surface and 150 m (Fig. 2) from the mean subsurface water concentration (mol m^{-3}), multiplying them by 10 and add them all together. The deficits are plotted versus Julian day and annual functions are manually fitted to the deficits of nitrate and C_T (Fig. 5). These functions are used in the further evaluation.

The model describes the volumetric enhancement of nitrate in the surface water (SW) during winter time, and is based on a mixed layer model

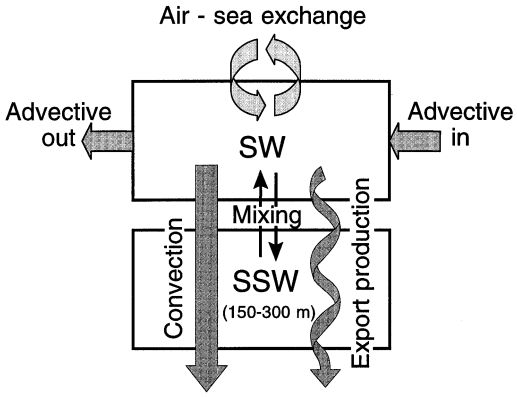

Fig. 4. Schematic illustration of the processes considered in the model used for the evaluation, where SW equals the surface water (0–150 m depth) and SSW equals the subsurface water (150–300 m depth).

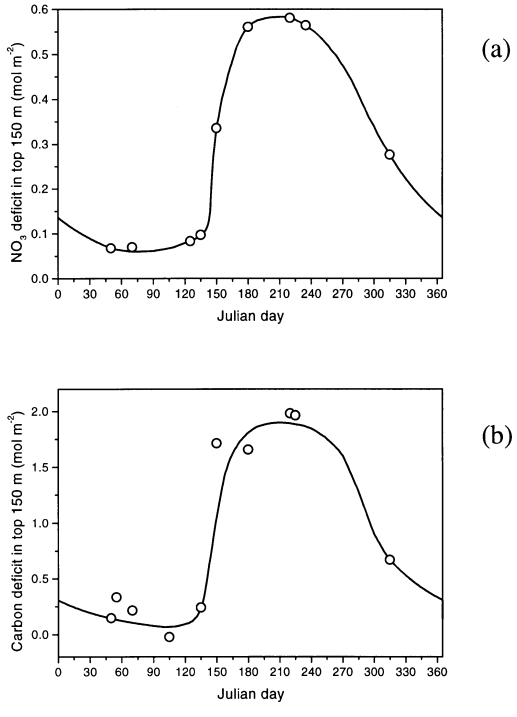

Fig. 5. The deficit of (a) nitrate and (b) C_T in the top 150 m (relative to the mean concentration in the depth range 150–300 m). The points represent the data from the different cruises, except for the one at Julian day 315, which is computed from two cruises as mainly surface water data are available from the Hákon Mosby, 1996 cruise. Lines have manually been fitted to the data points.

developed for idealised annual plankton cycles (Evans and Parslow, 1985). If the thickness of the surface water (SW) is H (m), the evolution of H is expressed by

$$\frac{dH}{dt} = m_v, \tag{1}$$

where t (d) is time, and m_v (m d^{-1}) is the rate of change of H. During winter H increases and $m_v > 0$. The average concentration of nitrate in the SW, N_{SW} (mmol m^{-3}), can then be expressed by the equation

$$\frac{dN_{SW}}{dt} = \frac{m_v}{H}(\overline{N_{SSW}} - N_{SW}), \tag{2}$$

where $\overline{N_{SSW}}$ (mmol m^{-3}) is the mean subsurface water (SSW) nitrate concentration over the depth interval 150 to 300 m.

The nitrogen deficit D_N (mmol m^{-2}) is defined as the difference between the mean subsurface concentration and the surface water concentrations of nitrate, according to

$$D_N = \int_{z=0}^{150} (\overline{N_{SSW}} - N_{SW})\, dz. \tag{3}$$

Since the subsurface concentration of nitrate is relatively constant during winter, we have that

$$\frac{d\overline{N_{SSW}}}{dt} \approx 0. \tag{4}$$

Eq. (2) can hence be put in the form

$$\frac{dD_N}{dt} \approx -\frac{m_v}{H} D_N. \tag{5}$$

If one considers the deficit of nitrogen over the uppermost 150 m of the water column, eq. (5) can be expressed as:

$$\frac{dD_N}{dt} \approx -\frac{m'_v}{150} D_N, \tag{6}$$

where m'_v (m d^{-1}) is a modified (or scaled) rate of change of H given by

$$m'_v = m_v \frac{150}{H}, \tag{7}$$

m'_v, can be determined directly from eq. (6)

$$m'_v \approx -\frac{150}{d^{end} - d^{start}} (\ln D_N^{end} - \ln D_N^{start}), \tag{8}$$

where d^{start} and d^{end} are the starting and ending

day of integration with nitrogen deficits D_N^{start} and D_N^{end}, respectively.

We have used the time period from Julian day 315 to Julian day 50 to determine m'_v ($d^{end} - d^{start} = 100$ days). This time period has been chosen since biological activity should be at minimum at this time of the year (Sverdrup, 1953), so changes in the surface water concentration of nitrate is mainly governed by deepening of the surface layer. Furthermore, it is the period from the latest measurements in the fall to the earliest in the winter. It is found that a daily increase in H corresponding to $m'_v = 2.1$ m d^{-1} is needed to decrease the deficit as shown in Fig. 5 from 0.276 mol m^{-2} at day 315, to 0.067 mol m^{-2} at day 50.

Following this we apply the obtained value of m'_v to both the nitrate and C_T functions when the density stratification is less than 0.1 sigma units, that is from day 328 to day 158, as evaluated from the T–S properties in the top 200 m (covering the interface between the surface and the subsurface waters). When the density gradient is larger, a constant background mixing is assumed.

The background mixing velocity m'_v during the stratification period is not easily determined. However, for a tracer concentration C (mol m^{-3}), m'_v can be expressed as (Smolarkiewicz, 1983)

$$m'_v = \frac{K_v}{C}\frac{\partial C}{\partial z}, \tag{9}$$

where K_v (m^2 s^{-1}) is the vertical mixing coefficient, and $\partial C/\partial z$ denotes the change of C over a vertical distance z (m). From Fig. 2a, we have that for the uppermost 150 m of the water column, $\partial NO_3/\partial z$ can be approximated as 10/150 μmol l^{-1} m^{-1}, and that a typical (mean) value of nitrate is 6 μmol l^{-1}. Therefore, for K_v equal to $1 \cdot 10^{-4}$ m^2 s^{-1} (Drange, 1994), we get that m'_v is 0.1 m d^{-1}. This value is similar to the value used by Fasham et al. (1990) for zero-dimensional ecosystem modelling in the North Atlantic. Based on the uncertainties involved in determining m'_v, we consider m'_v to be bracketed by 0.05 m d^{-1} and 0.2 m d^{-1}, with the value 0.1 m d^{-1} as our base case.

The time period with density difference less than 0.1 unit is longer than the time period used to evaluate the vertical mixing, biological activity occurs towards the end of this period. In the spring the nitrate and C_T concentrations decrease before the density gradient develops, which is likely the result of a combination of local primary production and occational mixing events (see Eilertsen (1993) and Towsend et al. (1992) for a discussion of phytoplankton spring blooms in the absence of stratification).

The daily flux of nitrate and C_T to the surface water by vertical mixing is computed using the above value of m'_v for the different time periods and the deficit functions of Fig. 5. The change in the fitted nitrate deficit, from one day to the next, that is not caused by vertical mixing, is attributed to biological processes, assuming that no other process affects this concentration. This computation can not be performed using the C_T function, as also air–sea flux effects it. The daily change in nitrate deficit is converted to carbon equivalents by using a C/N ratio of 7.5 as measured in organic matter collected in the Greenland Sea (Rey, unpublished data). The corresponding change in carbon units does thus represent the net effect of biological production and decay in the surface water.

The daily flux of carbon caused by vertical mixing and biological activity is shown in Fig. 6. As seen a significant flux of carbon from below occurs in the spring before stratification builds up. This vertical flux of carbon is a function of the mixing rate and the difference in carbon concentration between the surface and subsurface water. The relatively high flux in the spring is a result of the fact that the increase in C_T deficit starts around day 140 (Fig. 5b), while the stratification, hampering the vertical mixing, does not start until day 158, see above. For the same reason the flux increases in the fall (around day 330) when the stratification breaks down. The discontinuity in the vertical flux in Fig. 6 is a result of the simplified mixing formulation applied, see above.

The flux due to biological activity in Fig. 6 shows a strong negative peak associated with the spring bloom around day 140 and the production continues to be larger than the decay to around day 200, after which the flux gets positive when the decay of organic matter is larger than the productivity. Adding the fluxes over the year results in a flux of 11 g C m^{-2} yr^{-1} from below and an export production of 34 g C m^{-2} yr^{-1}. The annual export production is computed from the nitrate consumed in the surface water. As the only source of nitrate in our computation is the vertical

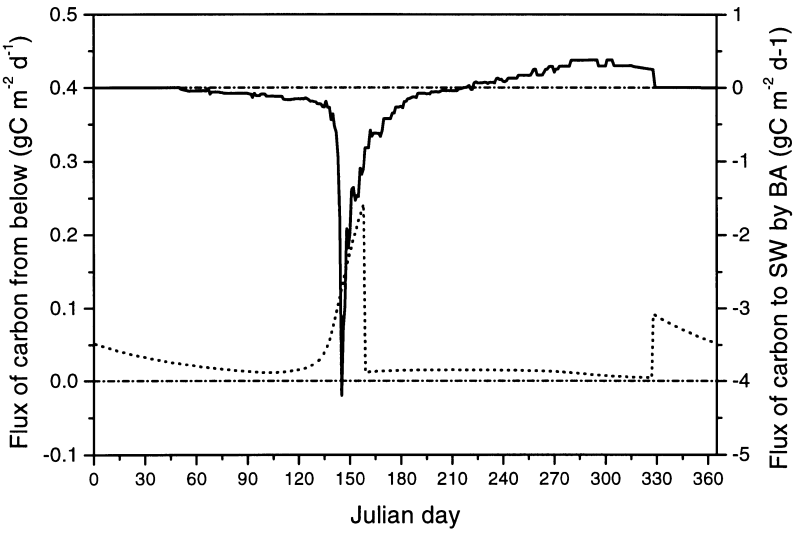

Fig. 6. The computed daily flux of carbon into the surface water (SW), caused by mixing from below (dotted line) and by biological activity (BA) (solid line). Note the order of magnitude difference in the two scales.

mixing, the annual export production is proportional to the flux of nitrate from below.

If the computed fluxes are assumed to be constant in the open deep Greenland Sea, we can compute the total flux by subtracting the ice covered part of the deep Greenland Sea area of 0.36×10^{12} m^2 (dotted line in Fig. 1). In Fig. 7, the relative ice cover over this region is shown for the years 1993 to 1997 (Kalany et al., 1996), the period during which the carbon system was studied. When the daily variability of the ice cover for the years 1993 to 1997 are used together with the daily carbon fluxes (Fig. 6), the computed total fluxes equal $3.3 \pm 0.3 \times 10^{12}$ g C yr^{-1} from below and $10.4 \pm 1.6 \times 10^{12}$ g C yr^{-1} as export production. The stated uncertainty is a result of the variability in the ice cover over the period 1993 to 1997.

5. Air–sea exchange

The flux of CO_2 over the air–sea interface, F, is a function of the difference in fugacity and wind speed, plus some parameters related to the properties of the CO_2 gas, according to:

$$F = 0.31 u^2 K_0 \sqrt{\frac{660}{\mathrm{Sc}}}\, \Delta f\mathrm{CO}_2, \qquad (10)$$

where K_0 is the solubility of CO_2, u is the 10 m wind speed (synoptic NCAR/NCEP surface wind data), Sc is the Schmidt number and $\Delta f\mathrm{CO}_2$ is the difference in fugacity between the atmosphere and that of the very surface water (Wanninkhof, 1992). In our computation we have used the mean value in the top 30 m of the water column (see Section 3) and the $\Delta f\mathrm{CO}_2$ is always positive and largest during the productive summer (Fig. 3b). However, during the winter the wind is stronger (Fig. 3c), resulting in a variable flux over the year but with no clear trend (Fig. 8). The short time variability is mainly caused by the variable wind field.

The daily fluxes presented in Fig. 8 are the averages $\pm$ the standard deviations caused by the wind for the years 1993 to 1997. The atmospheric $f\mathrm{CO}_2$ record used for the different years is the annual record of 1992 at weather station "Mike" (Conway et al., 1994) plus 1.6 μatm per year in order to compensate for the build up of atmospheric CO_2 by anthropogenic emissions. The small error in the atmospheric record by this approach is negligible in relation to the $\Delta f\mathrm{CO}_2$, which is in the range 50 to 100 μatm.

The summarized air–sea flux over the years 1993 to 1997 adds up to 52.9 ± 3.5 g C m^{-2} yr^{-1}, which represents the averaged flux in the open

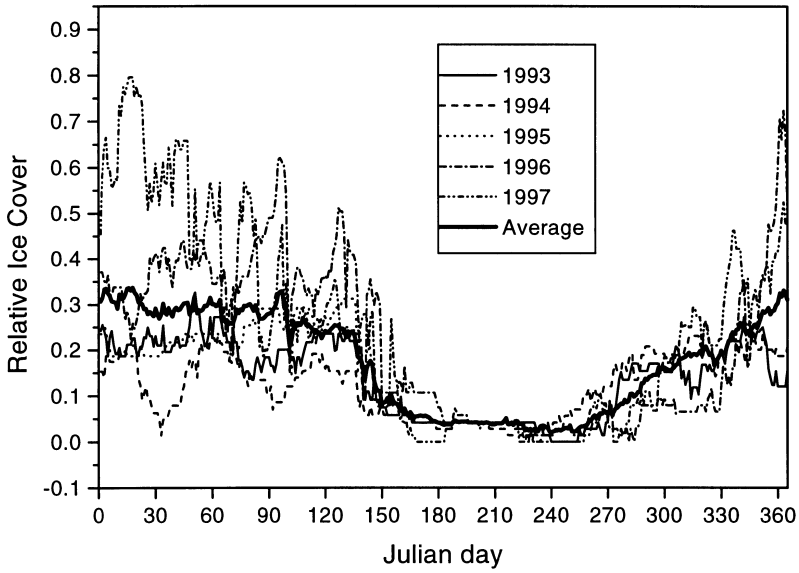

Fig. 7. The relative ice cover of the deep Greenland Sea for the years 1993 to 1997. The full line represents the annual average ice cover for this time period.

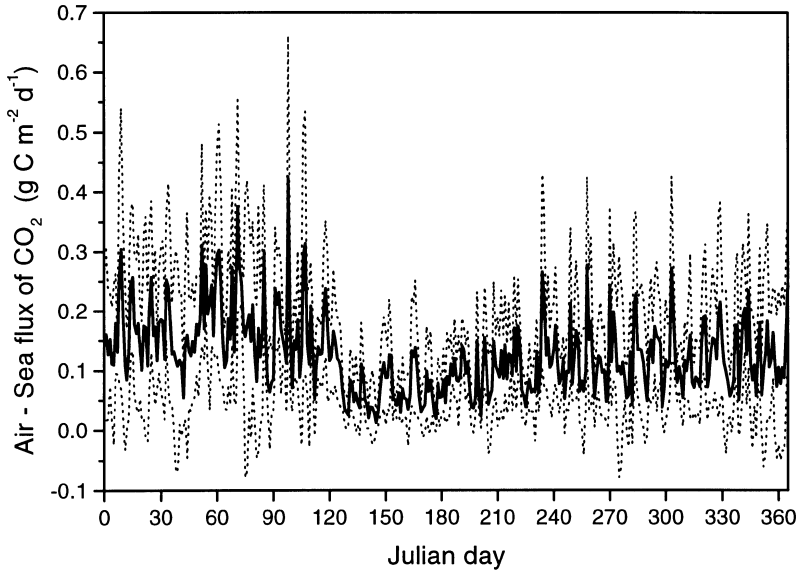

Fig. 8. The daily flux of CO_2 from the atmosphere to the sea, as computed from the surface wind for the years 1993 to 1997 and the difference in fugacity over the air–sea interface. The atmospheric fCO_2 record is corrected to correspond to the year of the surface wind used.

ocean. This value agrees well with that estimate by Hood et al. (1999) of 55 g C m^{-2} yr^{-1}, based on a combination of buoy data and sea surface temperature relationships. Both estimates are based on the Wanninkhof (1992) formulation for gas exchange using synoptic wind.

Sea ice has to be considered when the total flux of carbon dioxide into the Greenland Sea is com-

puted as a large fraction of the region is covered by ice. A combination of the daily air–sea carbon dioxide flux (Fig. 8) and the daily open water area of the deep Greenland Sea (Fig. 7) for each of the years 1993 to 1997, results in an average annual flux of $15.4 \pm 1.4 \times 10^{12}$ g C. The error in this estimate is a combination of the variability in wind speed and sea ice cover during the period.

6. Uncertainties

The above calculations are based on several assumptions that give rise to uncertainties. The first and probably most critical is how much the measured data vary between the years and how well the fitted line of the annual deficit of nitrate and C_T represents an "average year"? This question can only be addressed by looking at how well the measured data follow a general trend in Fig. 5. As is obvious, the nitrate data fall close to the fit, while the C_T data show more scatter. The latter might be a result of both interannual variability and variability within the observed concentrations of one data set. The latter variability (illustrated in Fig. 3a) is another general error, which results in an uncertainty in the deficit estimates of approximately 10%. Hence, we conclude that the approach of combining the different years is acceptable as the largest error is caused by the uncertainty in the deficit estimates for each time period.

The nitrate deficit in the spring, before primary production occurs, is relatively constant (Fig. 5a). The computation of the entrainment of subsurface water into the surface water is directly related to this deficit as well as the starting deficit in the fall. The latter is based on one data set (Julian day 315) and will thus give a corresponding uncertainty in the vertical flux. As the annual export production is proportional to the vertical flux of nitrate (see Section 4), the uncertainty will also be reflected in this estimate. On the other hand a corresponding change of the vertical flux of C_T will result, and hence the relation of export production to vertical flux of C_T will not be significantly affected. For example, if the mixing during the summer season, $m'_v = 0.1$ m d^{-1}, is set to the bracketing values 0.05 m d^{-1} (2 m d^{-1}), the modelled biological production changes from 34 to 32 g C m^{-2} yr^{-1} (39 g C m^{-2} yr^{-1}), while the mixing of C_T up into the surface water changes from 11 to 10 g C m^{-2} yr^{-1} (13 g C m^{-2} yr^{-1}).

In the estimate of biological activity we have neglected atmospheric deposition of nitrogen, as well as all other species of nitrogen except nitrate in the water column. The first will underestimate the annual primary production, while the second will have a minor impact in the annual budget. However, if we had full control over all the nitrogen species, the shape of the deficit curve might have been slightly different, changing the flux distribution of carbon caused by biological activity.

The use of the measured C/N ratio of 7.5 is in the range of reported values between 7 and 8.5 for decay of organic matter (Jones et al., 1984; Takahashi et al., 1993; Anderson and Sarmiento, 1994; Wallace et al., 1995). Hence, the variability of the computed export production is about $\pm 10\%$ if this span of C/N ratios is considered. The above uncertainties for the export production and vertical mixing of C_T would add up to a total uncertainty of about 20%.

The computed air–sea flux of carbon dioxide is based on the formulation of Wanninkhof (1992) which includes some uncertainties. These uncertainties have been much debated (Liss and Merlivat, 1986; Watson et al., 1991; Wanninkhof, 1992; Keeling, 1993), and we do not go into any detailed discussion on this topic. We only stress that the computed values most likely include an uncertainty of at most a factor 2.

7. Summary and conclusions

The different computed fluxes are summarized in Table 2, where the horizontal flux is given to balance the budget. The largest absolute carbon flux to the surface water in the Greenland Sea is a result of the spring bloom around Julian day 140 (Fig. 9). The rest of the year the daily flux is fairly low, but is mainly into the surface water adding up to a total of 30 g C m^{-2} for the whole year.

The fluxes of carbon to the surface water of the Greenland Sea by different processes considered in our computations result in this build up of carbon in the surface water which is significantly larger than the uncertainties of the model computations. This build up must correspond to the net

Table 2. *A summary of the annual computed mean carbon fluxes to the surface water (SW) of the Greenland Sea (GS) during the years 1993 to 1997*

	Fluxes to the SW of the GS	
Process	g C m^{-2} yr^{-1}	10^{12} g C yr^{-1}
air–sea flux	52.9 ± 3.5[a]	15.4 ± 1.4[a]
export production	-34[b]	-10.4 ± 1.6[a]
vertical mixing of C_T	11.3[b]	3.3 ± 0.3[a]
summary	30 ± 8	8 ± 2[a]
horizontal flux[c]	-30 ± 8	-8 ± 2[a]
total	0	0

[a] The noted errors are only due to the variability in wind field and sea ice extent during the time period.
[b] Error is estimated to be in the order 20%, see text.
[c] Computed to balance the budget.

horizontal flux, in order to balance the budget for the surface water. A horizontal net flux corresponding to 30 g C m^{-2} yr^{-1} gives that the top 150 m of the outflowing water has a concentration of C_T that is 20 μmol kg^{-1} higher than that of the inflowing water. This increase of C_T is likely a result of that the outflowing water is colder than the inflowing and thus has a higher solubility of CO_2. Surface water in contact with the atmosphere at these latitudes will increase the concentration of dissolved inorganic carbon by close to 10 μmol kg^{-1} for each degree the water get colder, if it keeps the same relative CO_2 saturation. Hence, a temperature decrease of the surface water during its stay in the Greenland Sea of about 2°C will explain the computed carbon build up. Such a temperature change is about what has been observed during all seasons between the surface waters in the Norwegian Atlantic Current and those north east of Iceland (Gathman, 1986).

From the above it is concluded that our assumption that the horizontal in- and out-flux are balanced, does not hold for C_T. However, it is more likely that this is the case for nitrate, as nitrate does not have an atmospheric source or sink (at least marginal in this area). Furthermore, it is only for nitrate that the assumption is critical, as the computation of biological activity relies on no other sources or sinks than vertical mixing. The computations based on the C_T measurements are not affected by the imbalance in the horizontal fluxes.

The annual export production as estimated by this method is proportional to the addition of nitrate to the photic zone through vertical mixing. This vertical mixing also adds C_T to the surface water. The difference between the export production and addition of C_T from below, 23 g C m^{-2} yr^{-1}, is close to 50% of the air–sea exchange. Hence, the annual flux of carbon dioxide

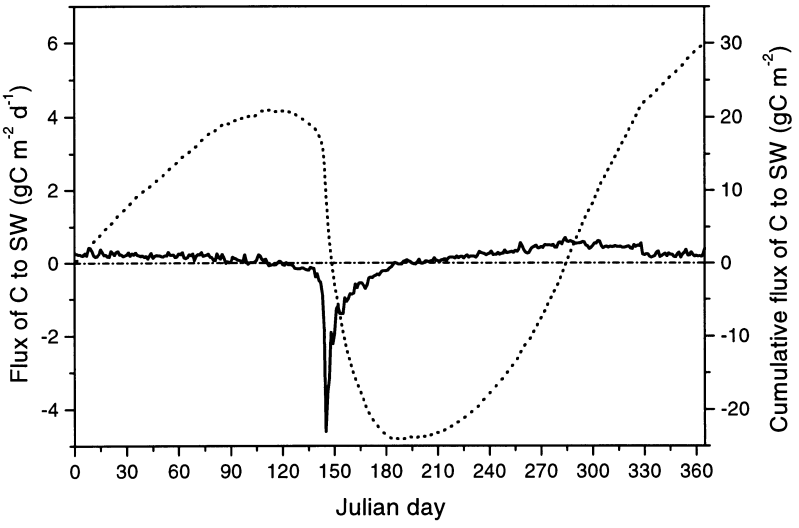

Fig. 9. A summary of the fluxes to the surface water (SW) over the year, both on a daily basis (solid line) and cumulative (dotted line).

from the atmosphere into the surface water of the Greenland Sea is equally driven by heat exchange, lowering the surface water temperature and thus also increasing the solubility of carbon dioxide, and the biological primary production, lowering the surface water fCO_2. However, the primary production causes a larger decrease in the surface water fCO_2 than the heat loss does, but the corresponding difference in the gas exchange is reduced due to the relatively low wind speeds during the summer season.

The different fluxes (Table 2) are between 1.4 and 6.4 times larger than the sequestering of anthropogenic CO_2 deeper than 1500 m (Andreson et al., 1999). This sequestering is a result of the ventilation to these depths with water having an anthropogenic concentration of 36 μmol kg^{-1} and does not consider where the anthropogenic CO_2 was taken up by the surface ocean. In fact most of the anthropogenic CO_2 is taken up by the surface water outside the Greenland Sea. Hence, it is not possible to discuss the anthropogenic flux in relation with the ones evaluated in this work in any other way than to compare the numbers.

8. Acknowledgements

This work was supported by the Commission of the European Union under the contract MAS3-CT95-0015 of the MAST-3 programme, and by the Nordic Council of Ministers. We are grateful to Göran Broström and Kim Holmén for valuable comments to an earlier version of this manuscript.

REFERENCES

Anderson, L. A. and Sarmiento, J. L. 1994. Redfield ratios of remineralisation determined by nutrient data analysis. *Global Biogeochem. Cycl.* **8**, 65–80.

Anderson, L. G., Chierici, M., Fogelqvist, E. and Johannessen, T. 1999. Flux of anthropogenic carbon into the deep Greenland Sea. *J. Geophys. Res.*, in press.

Bönisch, G. and Schlosser, P. 1995. Deep water formation and exchange rates in the Greenland/Norwegian Seas and the Eurasian Basin of the Arctic Ocean derived from tracer balances. *Prog. Oceanog.* **35**, 12–52.

Bönisch, G., Blindheim, J., Bullister, J. L., Schlosser, P. and Wallace, D. W. R. 1997. Long-term trends of temperature, salinity, density, and transient tracers in the central Greenland Sea. *J. Geophys. Res.* **102**(C8), 18,553–18,571.

Carlson, C. A., Ducklow, H. W. and Michaels, A. F. 1994. Annual flux of dissolved organic carbon from the euphotic zone in the northwestern Sargasso Sea. *Nature* **371**, 405–408.

Conway, T. J., Tans, P. P. and Waterman, L. S. 1994. Atmospheric CO_2 records from sites in the NOAA/CMDL air sampling network. In: *Trends '93: A compendium of data on global change* (eds. T. A. Boden, D. P. Kaiser, R. J. Sepanski and F. S. Stass). ORNL/CDIAC-65. Carbon Dioxide Information Analysis Center, Oak Ridge National Laboratory, Oak Ridge, TN, USA, 41–119.

Dickson, A. G. and Goyet, C. 1994. *Handbook of methods for the analysis of the various parameters of the carbon dioxide system in seawater*. Version 2. Report ORNL/CDIAC-74, Oak Ridge National Laboratory, Oak Ridge, TN, USA.

Drange, H. 1994. *An isopycnic coordinate carbon cycle model for the north Atlantic; and the possibility of disposing of fossil fuel CO_2 in the ocean.* PhD Thesis, Nansen Environm. Remote Sensing Center and Dept. Math., Univ. Bergen, Bergen, Norway.

Eilertsen, H. C. 1993. Spring blooms and stratification. *Nature* **363**, 24, 1993.

Evans, G. T. and Parslow, J. S. 1985. A model of annual plankton cycles. *Polar. Oceanogr.* **3**, 327–347.

Fasham, M. J. R., Duklow, H. W. and McKelvie, S. M. 1990. A nitrogen-based model of phytoplankton dynamics in the oceanic mixed layer. *J. Mar. Res.* **48**, 591–639.

Gathman, S. G. 1986. Climatology. In: *The Nordic seas* (ed. B. G. Hurdle). Springer-Verlag, New York, pp. 1–18.

Grasshoff, K. 1983. Determination of nitrate. In: *Methods of seawater analysis*, 2nd edition (eds. K. Grasshoff, M. Ehrhardt, and K. Kremling). Verlag Chemie GmbH, Weinheim, pp. 143–150.

Haraldsson, C., Anderson, L. G., Hassellöv, M., Hult, S. and Olsson, K. 1997. Rapid, high-precision potentiometric titration of alkalinity in ocean and sediment pore waters. *Deep-Sea Res.* **44**, 2031–2044.

Hood, E. M., Merlivat, M. and Johannessen, T. 1999. Variations of fCO_2 and air–sea flux of CO_2 in the Greenland Sea gyre using high-frequency time series data from CARIOCA drift buoys. *J. Geophys. Res.* **104**, 20,571–20,583.

Johnson K. M, King, A. E. and Sieburth, J. M. 1985. Coulometric TCO_2 analyses for marine studies: an introduction. *Mar. Chem.* **16,** 61–82.

Johnson K. M, Sieburth., J. M., Williams, P. J. and Brandstrom, L. 1987. Coulometric total carbon dioxide analysis for marine studies: automation and calibration. *Mar. Chem.* **21,** 117–133.

Jones, E. P., Dyrssen, D. and Coote, A. R. 1984. Nutrient regeneration in deep Baffin Bay with consequences for measurements of the conservative tracer NO and fossil fuel CO_2 in the oceans. *Can. J. Fish. Aquat. Sci.* **41**, 30–35.

Kalnay, E., Kanamitsu, M., Kistler, R., Collins, W., Deaven, D., Gandin, L., Iredell, M., Saha, S., White, G., Woollen, J., Zhu, Y., Chelliah, M., Ebisuzaki, W., Higgins, W., Janowiak, J., Mo, K. C., Ropelewski, C., Leetmaa, A., Reynolds R. and Jenne, R. 1996. The NCEP/NCAR reanalysis project. *Bull. Amer. Meteor. Soc.* **77**, 437–471.

Keeling, R. F. 1993. On the rôle of large bubbles in air–sea gas exchange and supersaturation in the ocean. *J. Mar. Res.* **51**, 237–271.

Lewis, E. and Wallace, D. W. R. 1998. *Program developed for CO_2 system calculations.* ORNL/CDIAC-105. Carbon Dioxide Information Analysis Center, Oak Ridge National Laboratory, U. S. Department of Energy, Oak Ridge, Tennessee.

Liss, P. S. and Merlivat, L. 1986. Air–sea gas exchange: introduction and synthesis. In: *The rôle of air–sea exchange in geochemical cycling* (ed. P. Buat-Ménard). Reidel, Dordrecht, pp. 113–127.

Noji, T. T., Rey, F., Miller, L. A., Børsheim, K. Y., Hirsche, H.-J. and Urban-Rich, J. 1996. Plankton dynamics and sedimentation. In: *European subpolar ocean programme: sea ice–ocean interaction* (eds. P. Wadhams, J. P. Wilkinson, S. C. S. Wells). Scott Polar Research Institute, University of Cambridge, UK, pp. 540–554.

Redfield, A. C., Ketchum, B. H. and Richards, F. A. 1963. The influence of organisms on the composition of sea water. In: *The sea*, Vol. 2 (ed. M. N. Hill). John Wiley, NY, pp. 26–77.

Rhein, M. 1991. Ventilation rates of the Greenland and Norwegian Seas derived from the distribution of the chlorofluoromethanes F-11 and F-12. *Deep-Sea Res.* **38,** 485–503.

Schlosser, P., Bönisch, G., Rhein, M. and Bayer, R. 1991. Reduction of deepwater formation in the Greenland Sea during the 1980s: evidence from tracer data. *Science* **251,** 1054–1056.

Siegenthaler, U. and Sarmiento, J. L. 1993. Atmospheric carbon dioxide and the ocean. *Nature* **365**, 119–125.

Smolarkiewicz, P. 1983. A simple positive definite advection scheme with small implicit diffusion. *Mon. Weather Rev.* **111**, 479–486.

Stocker, T. F., Broecker, W. S. and Wright, D. G. 1994. Carbon uptake experiments with a zonally-averaged global ocean circulation model. *Tellus* **46**, 103–122.

Sverdrup, H. U. 1953. On conditions for vernal blooming of phytoplankton. *J. Cons. Perm. Int. Explor. Mer.* **18**, 287–295.

Takahashi, T., Olafsson, J., Goddard, J. G., Chipman, D. W. and Sutherland, S. C. 1993. Seasonal variation of CO_2, and nutrient salts over the high latitude oceans: a comparative study. *Global Biogeochem. Cycl.* **7**, 843–878.

Townsend, D. W., Keller, M. D., Sieracki, M. E. and Ackleson, S. G. 1992. Spring phytoplankton blooms in the absence of vertical water column stratification. *Nature* **360**, 59–62.

Volk, T. and Hoffert, M. I. 1985. Ocean carbon pumps: analysis of relative strengths and efficiencies in ocean-driven atmospheric CO_2 changes. In: *The carbon cycle and atmospheric CO_2: natural variations archean to present* (eds. E. T. Sundquist, W. S. Broecker). American Geophysical Union, Washington, DC, pp. 99–110.

Wallace, D. W. R., Minnett, P. J. and Hopkins, T. S. 1995. Nutrients, oxygen, and inferred new production in the northeast water polynya, 1992. *J Geophys. Res.* **100**, 4323–4340.

Wanninkhof, R. 1992. Relationship between wind speed and gas exchange over the ocean. *J. Geophys. Res.* **97**, 7373–7382.

Watson, A. J., Upstill-Goddard, R. C. and Liss, P. S. 1991. Air–sea exchange in rough and stormy seas measured by a dual-tracer technique. *Nature* **349**, 145–147.